Fast and Precise Temperature Control for a Semiconductor Vertical Furnace via Heater-Cooler Integration

Wataru Ohnishi, *Member, IEEE*, Akira Hirata, Ryosuke Shibatsuji, and Tatsuya Yamaguchi

***Abstract*—Semiconductor vertical furnaces must achieve even faster and more precise temperature control due to the demand for ever-reducing the minimum feature size or critical dimension in semiconductor chips. Also, the insulation performance of vertical furnaces has improved to reduce power consumption; as a side effect, temperature reduction operation takes longer without active cooling. Therefore, in addition to heaters, vertical furnaces equipped with coolers have emerged to achieve higher productivity, more precise temperature control, and lower power consumption. However, the inability to generate positive and negative control inputs for one of the heaters or coolers poses a challenge for an intuitive controller parameter design. The aim of this paper is to address these issues by proposing an intuitive method for designing a controller in the frequency domain which virtually integrates heaters and coolers. We implemented the controller in a full-scale actual semiconductor vertical furnace and first confirmed that the linearity is high. Furthermore, we experimentally verified that the controller achieves both high-speed, high-precision temperature control and low power consumption.**

***Index Terms*—Feedforward control, feedback control, semiconductor vertical furnaces, temperature control, semiconductor manufacturing, system identification.**

I. Introduction

Semiconductor technology is the basis for the affluence and convenience of the modern world and plays an important role in a low-carbon society. Due to the demand for exponential improvements in computing power thanks to the shrinking of circuit critical dimensions and the introduction of 3-dimensional integrated circuits [1], [2], [3], the requirements for accuracy, productivity, and yield in semiconductor manufacturing processes increase year by year [4]. Thermal processing in semiconductor furnaces is an important process that involves oxidation, annealing, diffusion, or chemical vapor deposition. However, due to the long process time in the semiconductor manufacturing process [5], reducing the thermal budget [6] by fast temperature increase and decrease and short settling time[1] is necessary. Furthermore, the required temperature control accuracy is increasing [8] with the trend of shrinking circuit critical dimension.

The modeling of semiconductor furnaces has been studied using both physical modeling [9], [10], [11] and system identification [12], [13], [14]. A wide range of control methods have been applied to temperature control of vertical furnaces, including frequency-domain and time-domain designs. Frequency domain based feedback controller design includes Proportional-Integral-Differential (PID) control [15], [16], [17], [18], [19], frequency domain loop shaping [20], [21], decentralized control [22], and H_∞ control [24]. These methods have the advantage that the design of controller gain parameters is intuitive because the stability margin and control bandwidth are illustrated by Bode and Nyquist diagrams. Frequency domain design is often applied to single-input, single-output (SISO) systems, among which decentralized control and H_∞ control are applicable to multi-input, multi-output (MIMO) systems. Time domain based feedback controller design includes Linear Quadratic Gaussian (LQG) [14], [23], model predictive control (MPC), and internal model control [25]. LQG and MPC based on the state-space method can be easily extended to MIMO systems and has the advantage that the control law can be systematically determined by optimization. On the other hand, it is challenging to accurately model the plant as an MIMO system, and the design of weighting functions for optimization is less intuitive especially for higher-order systems. In addition to these feedback controllers, feedforward controller based on the model inverse system [14], [26] is effective in improving reference tracking performance. Furthermore, iterative learning control [27], [28], [29] is effective for reference tracking for repetitive tasks.

Although a substantial amount of research has been conducted on rapid and precise thermal control in terms of time- or frequency-domain designs and linear or nonlinear controllers, a limited amount of research has been conducted on fast settling at the set-point and temperature descent control that is highly coordinated with coolers. One reason for this is that some furnaces do not have cooling fans [17], [24] and cooling is sometimes performed naturally without control [24]. In contrast, vertical furnaces with active cooling systems with blowing fans have been proposed [30], [31] to achieve both energy savings by improving furnace insulation [32] and

Manuscript received 18 August 2022; revised 16 November 2022 and 17 December 2022; accepted 3 January 2023. Date of publication 11 January 2023; date of current version 5 May 2023. *(Corresponding author: Wataru Ohnishi.)*

Wataru Ohnishi is with the Department of Electrical Engineering and Information Systems, Graduate School of Engineering, The University of Tokyo, Tokyo 113-8656, Japan (e-mail: ohnishi@ieee.org).

Akira Hirata, Ryosuke Shibatsuji, and Tatsuya Yamaguchi are with the Thermal Control Engineering Department, Tokyo Electron Technology Solutions Ltd., Yamanashi 407-8511, Japan.

Color versions of one or more figures in this article are available at https://doi.org/10.1109/TSM.2023.3235492.

Digital Object Identifier 10.1109/TSM.2023.3235492

[1]The time after which the output remains within $\pm\varepsilon\%$ of its final value [7].

This work is licensed under a Creative Commons Attribution 4.0 License. For more information, see https://creativecommons.org/licenses/by/4.0/

throughput of temperature control. When both heaters and coolers are used, MIMO control methods, including LQG control, are often applied [23]. However, the presence of multiple pairs of control inputs to achieve the same heat input leads to simultaneous heater and cooler outputs, which increases power consumption. This is unavoidable unless an explicit switching mechanism is introduced. Another challenge is that the parameter design of LQG in the time domain is not intuitive.

The aim of this paper is to propose a control system design method in which the heater and cooler are virtually regarded as a single actuator, and the controller is designed to output both positive and negative signals. This allows for loop shaping in the frequency domain, which makes the tuning of the control system design intuitive. Also, it prevents the heater and cooler from being driven simultaneously, which results in the reduction of power consumption. Using the frequency response function (FRF) measurements via frequency-domain system identification [33], the proposed method integrates the heater and cooler with a constant gain. Furthermore, the effective use of the cooler is beneficial not only for decreasing but also for increasing the temperature, so that the temperature can be settled with less overshoot, even when the temperature is raised at high speed.

The experimental results obtained by using a full-scale vertical furnace demonstrated the effectiveness of the proposed controller design methodology in terms of fast settling and less overshoot. The results also showed that the presented switching control between the heater and cooler consumed less power than the LQG control, which drove both simultaneously. Also, nonlinear distortion analysis by using periodic excitation signals confirmed that linearity was sufficiently dominant, even when switching the heater and cooler. In summary, we present a high-performance controller design method for semiconductor vertical furnaces equipped with both heaters and coolers.

II. Experimental Setup

Fig. 1 shows a tall, highly productive vertical furnace capable of batch-wise heat treatment of approximately 100 silicon wafers of 300 mm diameter simultaneously [24], [34], [35]. The experimental setup utilized in this paper is a modified model of TELINDY PLUS™ manufactured by Tokyo Electron Technology Solutions Ltd. The vertical furnace is equipped with heaters and coolers, as shown in Fig. 2; hence, it can quickly decrease the temperature [16], [30]. For the temperature measurement, it has several thermocouples (TCs), one called outer TCs near the heater and the other called inner TCs in the process tube near the wafers. In addition, the vertical furnace is divided into 6 zones, but since this paper focuses on the integration of the heater and cooler, the average temperature of the inner TCs is used as the temperature output. Similarly, for the heaters and coolers, the respective average outputs are considered as inputs to the plant. Therefore, this paper treated the system as a two-input, one-output system with the average power of the heaters and coolers as input and the average inner temperature as output.

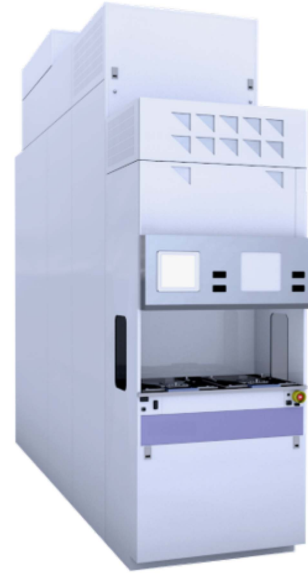

Fig. 1. Photo of the semiconductor vertical furnace.

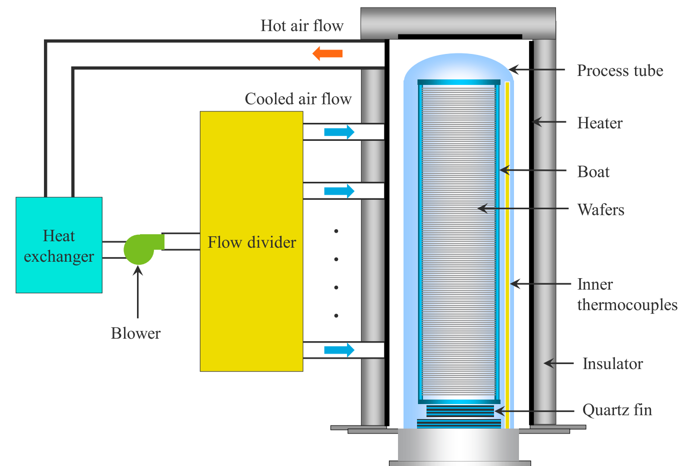

Fig. 2. Longitudinal cross-sectional view of the furnace with heaters, coolers, and inner thermocouples.

A. Control Problem Formulation

The purpose of temperature control in vertical furnaces is to improve the productivity and temperature control accuracy because of shrinking circuit critical dimensions. The following summarizes the performance requirements to be met by the designed controller:

R1 High linearity

The proposed method involves switching between heater and cooler. Therefore, a high linearity maintained even with such switching is desirable because the controller tuning in frequency domain is intuitive. In this paper, the required specification for nonlinear distortion analysis is that the excited harmonics must be at least 10 dB higher than the nonexcited harmonics.

R2 Short temperature settling time

To increase the throughput of the vertical furnace, the temperature settling time should be short. In this paper, the required specification is that the settling time at

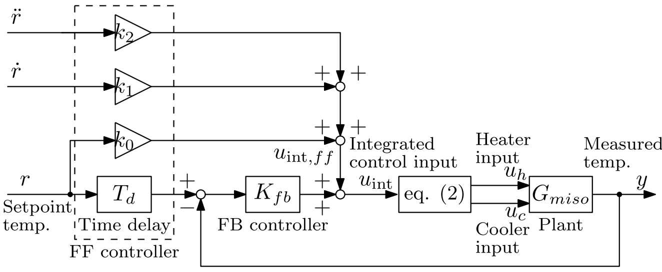

Fig. 3. Block diagram of the presented controller.

the transition between 300 and 400 degrees should be within 25 minutes for the temperature rise and within 50 minutes for the temperature fall.

R3 Less overshoot
To minimize circuit defects, the temperature overshoot should be small. In this paper, the required specification is to suppress the temperature overshoot to within 1 degree.

R4 Low power consumption
Reducing the power consumption of the furnace ideally involves not driving the heater and cooler at the same time. In this paper, the less power consumption is desirable in the conditions satisfying R1–R3.

III. Controller Design Based on Heater-Cooler Integration

The goal of this paper is to design a control system that satisfies R1–4 by using temperature control from 300°C to 400°C as an example. The temperature of 300°C is assumed to be the temperature at which silicon wafers are loaded, and 400°C is assumed to be the temperature at which deposition is performed on the silicon wafers. The experiment was conducted with 127 dummy silicon wafers in the vertical furnace.

Fig. 3 shows a configuration with 2 degrees of freedom control, i.e., a feedback controller responsible for disturbance suppression and a feedforward controller responsible for reference temperature tracking.

As described in Section II, the controlled vertical furnace is treated as a two-input, one-output system $G_{\mathrm{miso}} \in \mathcal{RH}_\infty^{2\times 1}$ with a heater input $u_h \in \mathbb{R}$, a cooler input $u_c \in \mathbb{R}$, and a temperature output $y \in \mathbb{R}$. Both u_h and u_c are expressed as a percentage of the maximum rating, and the unit for y is °C. Therefore, the input-output relationship is described by the following equation:

$$y = \underbrace{\begin{bmatrix} G_{h,T} & G_{c,T} \end{bmatrix}}_{G_{\mathrm{miso}},T} \begin{bmatrix} u_h \\ u_c \end{bmatrix}, \tag{1}$$

where T denotes the nominal operating temperature as °C.

First, the proposed method performs system identification in Section III-A to obtain the coefficients for heater-cooler integration. Section III-B describes the feedforward controller design and Section III-C describes the feedback controller design. Heater-cooler integration allows the integrated virtual actuator to produce positive and negative outputs, which makes the controller design more intuitive.

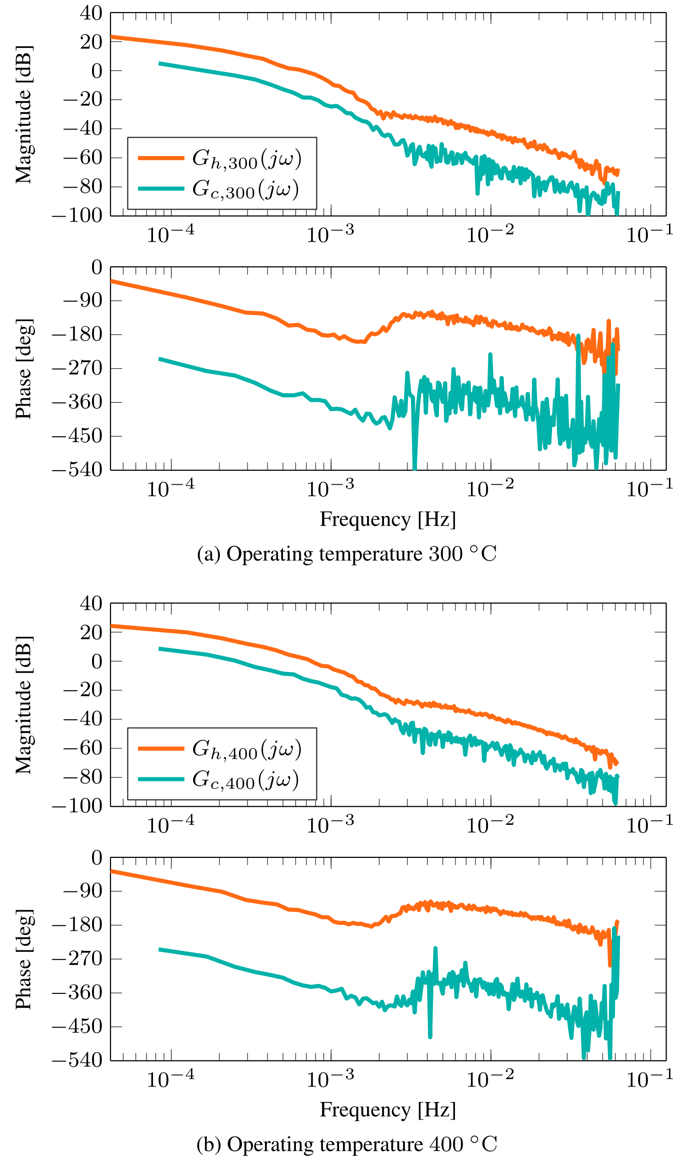

Fig. 4. Frequency response of the vertical furnace.

A. Frequency Response Measurement

The frequency response of the plant was measured using frequency domain system identification [33], [36] with zippered multisine signal. Fig. 4 shows the frequency characteristics obtained at approximately 300 °C and 400 °C. Fig. 4 indicates that the heater and cooler characteristics are similar, except for the phase reversal and gain offset. This result motivated the integration of a heater and cooler with a constant gain.

Also, the characteristics at 300 °C and 400 °C were not significantly different. Therefore, we set 400 °C degrees as the nominal conditions for the heater-cooler integration and feedforward controller design shown in Section III-B. In the feedback controller design shown in Section III-C, the union of FRFs for four conditions is considered to improve the robustness.

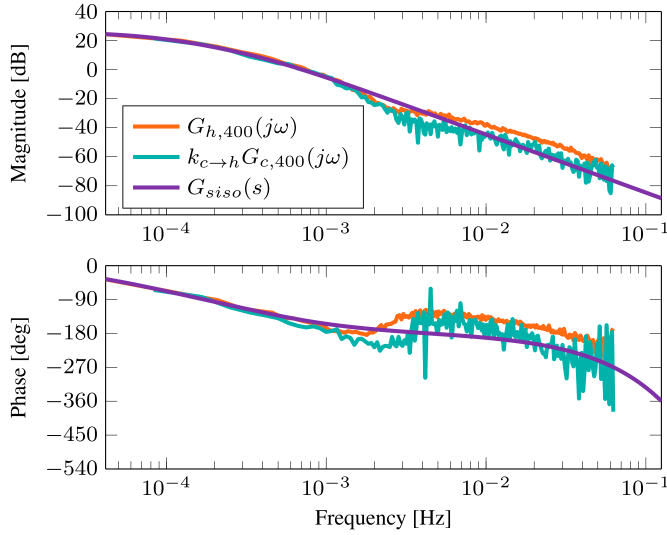

Fig. 5. Frequency response data and second-order model after the presented heater-cooler integration.

B. Heater/Cooler Integration and Parametric Modeling

This section presents the heater-cooler integration method. The integrated control input u_{int} by (2) generates the heater power u_h and cooler power u_c:

$$\begin{cases} u_h = u_{\text{int}} & u_c = 0 & \text{if } u_{\text{int}} \geq 0 \\ u_h = 0 & u_c = \frac{1}{k_{c\to h}} u_{\text{int}} & \text{else} \end{cases} \tag{2}$$

In (2), $k_{c\to h} \in \mathbb{R}$ denotes a constant gain that brings the frequency response of the cooler $G_{c,T}(j\omega)$ closer to the frequency response of the heater $G_{h,T}(j\omega)$ focusing on the steady state, i.e., $\omega = 0$, as formulated in (3):

$$k_{c\to h} = \frac{G_{h,T}(0)}{G_{c,T}(0)} \tag{3}$$

Therefore, the heater-cooler integrated controlled system is obtained as follows

$$G_{\text{siso},T} = \frac{1}{2} G_{\text{miso},T} \begin{bmatrix} 1 \\ k_{c\to h} \end{bmatrix}. \tag{4}$$

In this paper, $T = 400$ [°C] is chosen as the nominal operating temperature and then $k_{c\to h} = -4.3921$ is obtained. Fig. 5 shows the heater-cooler integrated characteristics and a fitted second order transfer function $G_{\text{siso}}(s)$ as

$$G_{\text{siso}}(s) = e^{-4s} \frac{1}{4.34 \times 10^4 s^2 + 134s + 0.0518}, \tag{5}$$

in which s denotes the Laplace variable. Fig. 5 indicates that the cooler side characteristics shifted well to the heater side characteristics by multiplying $k_{c\to h}$.

As shown in Fig. 5, the dynamics of the system can be well modeled with the second-order system with a time delay. Therefore, the feedforward controller is also set to the second-order system and the dead time compensation, and the gains are determined by trial and error as follows.

$$u_{\text{int},ff} = 2.61 \times 10^4 \ddot{r} + 101\dot{r} + 0.00643r + 1.11 \tag{6}$$

$$T_d = e^{-4s} \tag{7}$$

C. Feedback Controller Design Based on Loop-Shaping

Discrete time PID controller is designed through the union of four conditions $[G_{h,400}(j\omega), G_{h,300}(j\omega), k_{c\to h}G_{c,400}(j\omega), k_{c\to h}G_{c,400}(j\omega)]$. Since the controller optimization problem is a nonlinear optimization problem, the PID gains are optimized through the following steps [37].

1) Optimization Problem Formulation: A PID controller with sampling time T_s and its tuning parameters $\boldsymbol{\rho}$ are formulated as

$$K_{fb}(z, \boldsymbol{\rho}) = k_p + k_i \frac{T_s}{z-1} + k_d \frac{1}{T_f + T_s/(z-1)}, \tag{8}$$

where $z = e^{T_s s}$ and $\boldsymbol{\rho} = [k_p, k_i, k_d, T_f]$, respectively. k_p, k_i, k_d, and T_f denote the proportional, integral, and derivative gains and the time constant of the pseudo derivative.

The upper limit of the gain of the sensitivity function $M_s = 2$ was set as a constraint in order to suppress the amplification of disturbances and to ensure a stability margin. Under this constraint, an optimization problem to improve the disturbance suppression performance in the low frequency range is formulated as follows.

$$\underset{\boldsymbol{\rho}}{\text{maximize}} \quad \Omega_{gc} \tag{9}$$

$$\text{subject to} \quad \left| \frac{\Omega_{gc}}{j\omega} \right|^m - |1 + L_{u,T}(j\omega, \boldsymbol{\rho})| \leq 0, \tag{10}$$

$$\frac{1}{M_S} - |1 + L_{u,T}(j\omega, \boldsymbol{\rho})| \leq 0, \tag{11}$$

$$0 \leq \boldsymbol{\rho}, \tag{12}$$

where

$$\begin{aligned} & u \in \{h, c\}, T \in \{300, 400\} \quad \text{and} \\ & L_{h,T}(j\omega, \boldsymbol{\rho}) = K_{fb}(j\omega, \boldsymbol{\rho}) G_{h,T}(j\omega) \\ & L_{c,T}(j\omega, \boldsymbol{\rho}) = K_{fb}(j\omega, \boldsymbol{\rho}) k_{c\to h} G_{c,T}(j\omega). \end{aligned} \tag{13}$$

Ω_{gc} indicates the feedback control bandwidth to be maximized. m represents the constraint in the low frequency range of the sensitivity function for disturbance suppression. In this paper, $m = 2$ was chosen.

2) Gain Parameter Optimization: Because the optimization problem formulated in (9)–(12) is nonlinear, the initial value given for the optimization solver highly affects the obtained local optimal gain. We applied the following step-by-step optimization to prepare the reasonable initial parameters:

1) Pole-placement design that uses the delay-ignored continuous-time second order nominal plant (5) [38]
2) Sequential linearization that uses the results of Step 1) as initial values
3) Nonlinear optimization that uses the results of Step 2) as initial values

For more details, refer to [37].

The designed feedback controller shown in Fig. 6 has the specified robustness in the four conditions. Furthermore, it can be seen that it has a control bandwidth of approximately 1×10^{-3}Hz.

TABLE I
ESTIMATED ENERGY CONSUMPTION COMPARISON IN 80 MINUTES [kWh]

	300[°C] to 400[°C]			400[°C] to 300[°C]		
	Heater	Cooler	Rise total	Heater	Cooler	Fall total
Optimal control (Heater only)	4.99	0.00	4.99	0.03*	0.00*	0.03*
Optimal control (Heater and cooler)	37.47	3.86	41.32	24.79	4.10	28.89
Proposed control (Heater-cooler integration)	6.02	0.13	6.15	2.04	0.63	2.67

* Settling time is significantly longer than the other two methods.

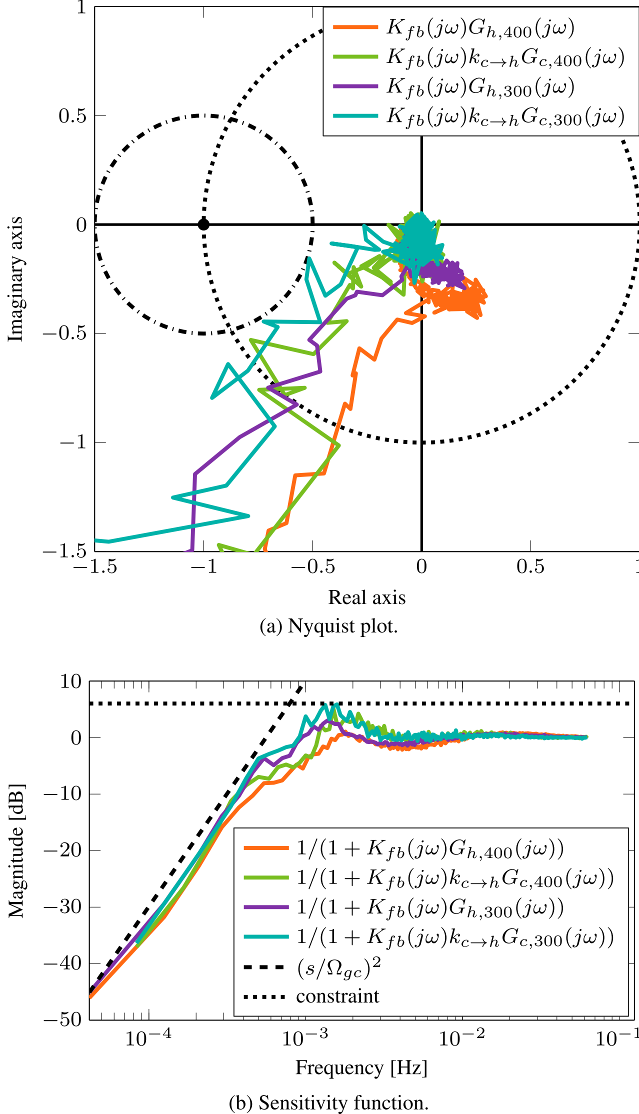

Fig. 6. Feedback controller design. The constraints are met in all four FRFs. (a) The Nyquist diagram showing the robustness. The Nyquist diagram outside the circle of radius 0.5 centered at $(-1, 0j)$ satisfies the constraint of the sensitivity function upper bound of $M_s = 2$. (b) Sensitivity function showing the disturbance suppression performance. It has a control bandwidth of approximately 10^{-3} Hz.

IV. EXPERIMENTAL RESULTS

This section verifies the effectiveness of the controller described in Section III.

First, Section IV-A discusses the high linearity from the integrated control input u_{int} to the temperature y by nonlinear distortion analysis by using multisine excitation, and the design requirement R1 is satisfied.

Furthermore, Section IV-B discusses an experiment on the temperature transition from 300 °C to 400 °C. The objective of the experiment is to demonstrate that the proposed method satisfies R2–4 with fast and accurate temperature control. We compared the experimental results with those obtained by using only the heater without the cooler, and the proposed method satisfies R2–3. Also, we compared the experimental results with those designed by LQG by using both the cooler and heater, and R4 is satisfied.

A. Nonlinear Distortion Analysis

The proposed method involves switching the heater and cooler control inputs, which can introduce nonlinear distortions. Therefore, we applied a multisine signal [33] to the integrated control input u_{int} and performed a nonlinear distortion analysis. The experiments were performed around 300 °C.

Fig. 7 shows the results of a nonlinear distortion analysis performed on the output signal of three different amplitude inputs normalized by the maximum power of the cooler. Unlike the Bode diagram, the output amplitude changes when the input amplitude is changed because it is not normalized by the input amplitude. For all three amplitudes, the excited odd harmonics are significantly larger than the nonexcited harmonics; thus, linearity dominates and R1 is satisfied. Therefore, using frequency response data to design a linear control system is reasonable. In addition, even harmonics have larger amplitude than odd harmonics, which may be because a fourth-order expression for temperature describes the leaving radiative flux [9], [11].

B. Temperature Control Results

We conducted three experiments: 1) LQG control by using only the heater without the cooler, 2) LQG control with the heater and cooler as separate actuators, and 3) the proposed control with the virtual integrated actuator. Fig. 8 shows the time response results, and Table I compares the estimated energy consumption for 80 minutes for each temperature rise and fall. Since the control inputs were recorded as a percentage of the maximum ratings, this value of energy consumption was estimated simply by integrating the linearly interpolated value from the maximum rated power.

1) LQG Control Using Only the Heater: Fig. 8(a) shows the results of the temperature control that uses only the heater without a cooler. A large overshoot occurs near the point in which the temperature changes from 300 °C to 400 °C because of the lack of a cooling control input; hence, R3 is not satisfied. Also, when the temperature is lowered from 400 °C to 300 °C,

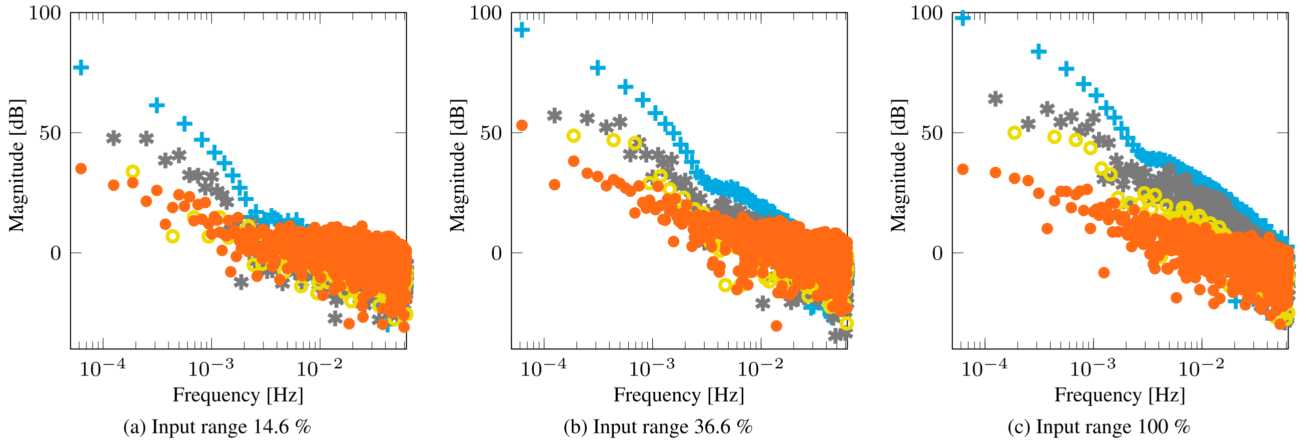

(a) Input range 14.6 % (b) Input range 36.6 % (c) Input range 100 %

Fig. 7. Nonlinear distortion analysis. +: excited odd harmonics, ✱: non-excited even harmonics, ○: non-excited odd harmonics, ●: noise variance. The excited odd harmonics are significantly larger than the nonexcited harmonics, indicating that linearity is dominant. R1 is satisfied.

(a) LQG control (Heater only) (b) LQG control (Heater and cooler) (c) Proposed control (Heater-cooler integration)

Fig. 8. Experimental results. The top graph shows the time response of the temperature control reference r and the actual temperature y. The second graph highlights the temperature rise in this top graph, and the third graph highlights the temperature fall in this top graph. The bottom graph shows the control inputs for the heater u_h and cooler u_c. The proposed method satisfies R2–4 because it has short temperature settling, less overshoot, and low power consumption. On the other hand, from (b) and (c), the waveforms of temperature rise and fall are not symmetrical, indicating that there is a temperature dependency in the plant.

the temperature drop occurs very slow because of the lack of active cooling; therefore, R2 is not satisfied. The improved insulation of the furnace to increase thermal efficiency causes this drawback [32].

2) LQG Control With Heater and Cooler: Fig. 8(b) shows the experimental results that used optimal control, in which the heater and cooler are considered separate actuators. Compared to Fig. 8(a), the use of the cooler in addition to the heater

reduces the overshoot at the temperature rise and speeds up the temperature fall, thus satisfying R2–3. However, because the control law is calculated with the heater and cooler as separate actuators, the heater and cooler are driven simultaneously to control the temperature at a constant level, hence R4 is not satisfied.

3) Proposed Control With the Virtual Integrated Actuator: The experimental results of the proposed method, shown in Fig. 8(c), indicate that R2–3 is satisfied because of the small overshoot and short settling time. Furthermore, the settling time during the rising temperature has become shorter compared to that in Fig. 8(b). Also, because the control law is based on actuator switching, as shown earlier in Table I, the energy consumption is significantly lower than that of the optimal control that used both the heater and cooler; thus, R4 is satisfied.

From the above, it is concluded that the proposed method has desirable characteristics satisfying R1–4.

Interestingly, both Fig. 8(b) and (c) show asymmetric temperature rise and fall waveforms. This implies that the closed-loop system has some degree of nonlinearity, which is the residue of the linearization effect of the feedback control. The reason for this nonlinearity is likely to be temperature dependency of the plant. Although the same gain could meet the R1–R4 for the 300°C and 400°C transitions, the introduction of feedback and feedforward controllers with a variable gain that explicitly takes temperature dependency into account would be effective for transitions over a wider temperature range.

V. Conclusion

This paper proposes a control method that virtually integrates a heater and cooler for a semiconductor vertical furnace, which requires faster, more accurate, and lower power consumption temperature control at the same time. With virtual actuator integration, the controller can output both positive and negative outputs, which allows for an intuitive controller design in the frequency domain. Although this method involves actuator switching, its linearity is sufficiently high, as demonstrated by nonlinear distortion analysis experiments. Experiments in an actual full-scale semiconductor vertical furnace have successfully achieved high speed, high accuracy, and low power consumption.

This technology is expected to reduce the number of man-hours required for future controller design while improving temperature control accuracy. Future work will include modeling the temperature dependence for wider range of temperature and learning control.

References

[1] G. Moore, “Cramming more components onto integrated circuits,” *Electron. Mag.*, vol. 38, pp. 114–117, Apr. 1965.

[2] H. Butler, “Position control in lithographic equipment,” *IEEE Control Syst. Mag.*, vol. 31, no. 5, pp. 28–47, Oct. 2011.

[3] M. Steinbuch, T. Oomen, and H. Vermeulen, “Motion control, mechatronics design, and Moore’s law,” *IEEJ J. Ind. Appl.*, vol. 11, no. 2, pp. 245–255, 2022.

[4] S. Shinde, A. Sonar, and Y. Sun, “Advanced process control for furnace systems in semiconductor manufacturing,” in *Proc. Adv. Semicond. Manuf. Conf.*, 2013, pp. 275–279.

[5] Y. Mikata, K. Tanimoto, K. Ishii, and S. Oka, “Improvement of minifab uptime by using multitask and multifunctional tools,” *IEEE Trans. Semicond. Manuf.*, vol. 17, no. 3, pp. 273–280, Aug. 2004.

[6] X. X. Zhang, H. X. Li, B. Wang, and S. Ma, “A hierarchical intelligent methodology for spatiotemporal control of wafer temperature in rapid thermal processing,” *IEEE Trans. Semicond. Manuf.*, vol. 30, no. 1, pp. 52–59, Feb. 2017.

[7] S. Skogestad and I. Postlethwaite, *Multivariable Feedback Control: Analysis and Design*. Chichester, U.K.: Wiley, 2005.

[8] A. Fischer, A. Routzahn, S. M. George, and T. Lill, “Thermal atomic layer etching: A review,” *J. Vac. Sci. Technol. A*, vol. 39, no. 3, 2021, Art. no. 30801.

[9] B. J. Van Schravendijk, W. L. De Koning, and W. C. Nuijen, “Modeling and control of the wafer temperatures in a diffusion furnace,” *J. Appl. Phys.*, vol. 61, no. 4, pp. 1620–1627, 1987.

[10] C. J. Huang, C. C. Yu, and S. H. Shen, “Selection of measurement locations for the control of rapid thermal processor,” *Automatica*, vol. 36, no. 5, pp. 705–715, 2000.

[11] Q. He, S. J. Qin, and A. J. Toprac, “Computationally efficient modeling of wafer temperatures in a low-pressure chemical vapor deposition furnace,” *IEEE Trans. Semicond. Manuf.*, vol. 16, no. 2, pp. 342–350, May 2003.

[12] K. Tsakalis and K. Stoddard, “Integrated identification and control for diffusion/CVD furnaces,” in *Proc. IEEE Symp. Emerg. Technol. Factory Autom.*, 1997, pp. 514–519.

[13] A. Theodoropoulou, R. A. Adomaitis, and E. Zafiriou, “Model reduction for optimization of rapid thermal chemical vapor deposition systems,” *IEEE Trans. Semicond. Manuf.*, vol. 11, no. 1, pp. 85–98, Feb. 1998.

[14] J. L. Ebert et al., “Model-based control of rapid thermal processing for semiconductor wafers,” in *Proc. Amer. Control Conf.*, vol. 5, 2004, pp. 3910–3921.

[15] S. Hirasawa, S. Kieda, T. Watanabe, T. Torii, T. Takagaki, and T. Uchino, “Temperature distribution in semiconductor wafers heated in a vertical diffusion furnace,” *IEEE Trans. Semicond. Manuf.*, vol. 6, no. 3, pp. 226–232, Aug. 1993.

[16] K. Nakao et al., “Multi-wafer rapid isothermal processing,” in *Proc. IEEE Int. Symp. Semicond. Manuf. Conf.*, 2001, pp. 145–148.

[17] M. Hattori, M. Okumura, and N. Niimi, “PID temperature control improvement of semiconductor furnace using fuzzy inference,” *Koyo Eng. J. English Ed.*, vol. 163, pp. 63–67, 2003. [Online]. Available: http://eb-cat.ds-navi.co.jp/enu/tech/ej/img/no163e/163e_13.pdf

[18] J. Gumpher, W. A. Bather, and D. Wedel, “LPCVD silicon nitride uniformity improvement using adaptive real-time temperature control,” *IEEE Trans. Semicond. Manuf.*, vol. 16, no. 1, pp. 26–35, Feb. 2003.

[19] A. J. Su, J. C. Jeng, H. P. Huang, C. C. Yu, S. Y. Hung, and C. K. Chao, “Control relevant issues in semiconductor manufacturing: Overview with some new results,” *Control Eng. Pract.*, vol. 15, no. 10, pp. 1268–1279, 2007.

[20] K. Tsakalis, J. J. Flores-Godoy, and K. Stoddard, “Temperature control of diffusion/CVD furnaces using robust multivariable loop-shaping techniques,” in *Proc. IEEE Conf. Decis. Control*, vol. 4, 1999, pp. 4192–4197.

[21] E. Grassi and K. Tsakalis, “PID controller tuning by frequency loop-shaping: Application to diffusion furnace temperature control,” *IEEE Trans. Control Syst. Technol.*, vol. 8, no. 5, pp. 842–847, Sep. 2000.

[22] C. D. Schaper, T. Kailath, and Y. J. Lee, “Decentralized control of wafer temperature for multizone rapid thermal processing systems,” *IEEE Trans. Semicond. Manuf.*, vol. 12, no. 2, pp. 193–199, May 1999.

[23] S. C. Shah and P. Pandey, “Thermal reactor optimization,” U.S. Patent 5 517 594, 1995.

[24] M. Tucker, E. Valdez, K. Tsakalis, M. Warren, and K. Stoddard, “Improving vertical furnace performance using model-based temperature control,” in *Proc. SEMI/SEMATECH AEC/APC Symp.*, 1998, pp. 1–6.

[25] C. Schaper, M. Moslehi, K. Saraswat, and T. Kailath, “Control of MMST RTP: Repeatability, uniformity, and integration for flexible manufacturing,” *IEEE Trans. Semicond. Manuf.*, vol. 7, no. 2, pp. 202–219, May 1994.

[26] A. Theodoropoulou, E. Zafiriou, and R. A. Adomaitis, “Inverse model-based real-time control for temperature uniformity of RTCVD,” *IEEE Trans. Semicond. Manuf.*, vol. 12, no. 1, pp. 87–101, Feb. 1999.

[27] K. S. Lee, J. Lee, I. Chin, J. Choi, and J. H. Lee, "Control of wafer temperature uniformity in rapid thermal processing using an optimal iterative learning control technique," *Ind. Eng. Chem. Res.*, vol. 40, no. 7, pp. 1661–1672, 2001.

[28] J. Y. Choi and H. M. Do, "A learning approach of wafer temperature control in a rapid thermal processing system," *IEEE Trans. Semicond. Manuf.*, vol. 14, no. 1, pp. 1–10, Feb. 2001.

[29] D. R. Yang, K. S. Lee, H. J. Ahn, and J. H. Lee, "Experimental application of a quadratic optimal iterative learning control method for control of wafer temperature uniformity in rapid thermal processing," *IEEE Trans. Semicond. Manuf.*, vol. 16, no. 1, pp. 36–44, Feb. 2003.

[30] A. Dip, R. Soave, S. Kaushal, K. Nakao, S. Sasaki, and T. Tsuda, "Rapid isothermal batch processing," in *Proc. 10th IEEE Int. Conf. Adv. Therm. Process. Semicond.*, 2002, pp. 39–46.

[31] K. Yoshii, T. Yamaguchi, W. Wang, and T. Saito, "Vertical-type heat treatment apparatus," U.S. Patent 9 255 736 B2, 2019.

[32] K. Yoshii, T. Yamaguchi, W. Wang, and T. Saito, "Vertical-type heat treatment apparatus, and control method for same," U.S. Patent 64 469 A1, 2012.

[33] R. Pintelon and J. Schoukens, *System Identification: A Frequency Domain Approach*, 2nd ed. Hoboken, NJ, USA: Wiley-IEEE Press, 2012.

[34] Y. Kunii, E. S. Nakashima, E. H. Miya, E. Hidehiro, and Y. N. Mise, "Vertical furnaces for thin film deposition and annealing contributing to low-cost, high-performance semiconductor device manufacturing," *Hitachi Rev.*, vol. 60, no. 5, pp. 193–197, 2011.

[35] S. Shinde, C. H. Chan, M. Minchew, and L. Mbonu, "Innovative approach on dynamic behavior of LPCVD nitride process on diffusion furnace: Equipment optimization/advanced process control/contamination free manufacturing," in *Proc. Adv. Semicond. Manuf. Conf.*, 2020, pp. 1–4.

[36] E. Evers, N. Van Tuijl, R. Lamers, B. De Jager, and T. Oomen, "Fast and accurate identification of thermal dynamics for precision motion control: Exploiting transient data and additional disturbance inputs," *Mechatronics*, vol. 70, Oct. 2020, Art. no. 102401.

[37] W. Ohnishi, "Data-based feedback controller tuning utilizing collocated and non-collocated sensors," in *Proc. Joint 8th IFAC Symp. Mechatronic Syst. 11th IFAC Symp. Nonlinear Control Syst.*, 2019, pp. 560–565.

[38] G. C. Goodwin, S. F. Graebe, and M. E. Salgado, *Control System Design*. Hoboken, NJ, USA: Prentice Hall, 2000.